J. Mech. Phys. Solids Vol. 37, No. 2, pp. 233–263, 1989.
Printed in Great Britain.

0022–5096/89 $3.00 + 0.00

ASYMPTOTIC FIELDS AT TIP OF CONICAL NOTCHES AND INCLUSIONS IN A POWER HARDENING SOLID

N. A. FLECK* and D. DURBAN†

*University Engineering Department, Trumpington Street, Cambridge CB2 1PZ, U.K.; and
†Department of Aeronautical Engineering, Technion, Haifa, Israel

(*Received* 15 *March* 1988)

ABSTRACT

THE asymptotic field is determined at the tip of a conical notch and of a rigid cone in an incompressible power law hardening solid, subjected to axisymmetric loading. For both geometries, no singularity exists with torsional loading, but singular solutions do exist with torsionless axisymmetric loading. For the conical notch, the level of strain singularity increases with an increase of the strain hardening exponent n, and is greatest when the included cone semi-angle α is between 0° and 60° depending upon n. For the rigid cone, the level of strain singularity increases with increasing n and decreasing α. Contours of constant effective stress and details of the stress components are given over a wide range of α and n, for both geometries.

1. INTRODUCTION

THE ASYMPTOTIC stress field near the tip of a sharp inhomogeneity of some prescribed shape in an elastic–plastic body may be singular in form. A well-known example is the singular field near the tip of a crack in a power law material, as found by HUTCHINSON (1968a, b), and by RICE and ROSENGREN (1968).

In this paper, asymptotic solutions are reviewed for the stress field near the tip of a two-dimensional (2D) notch or rigid wedge in a plane elastic body, and near the tip of a cone in a three-dimensional (3D) elastic body. A new solution is presented for the cases of a conical notch and rigid cone in an incompressible elastic body under torsion; no singularity is found. Solutions are also given for a conical notch and for a rigid cone in an incompressible power law material under torsionless axisymmetric loading; singular solutions exist, with the level of singularity depending upon the strain hardening exponent and the included apex angle 2α of the cone.

1.1. *The two-dimensional notch and rigid wedge*

The singular field at the tip of a stress free notch and of a rigid wedge in a plane elastic body has been investigated by WILLIAMS (1952) and by KARAL and KARP (1962, 1964) independently. Consider first the stress-free notch, of included apex angle 2α and wedge angle $\beta = 180° - \alpha$ (Fig. 1). The strain ε_{ij} varies with distance r from the apex according to $\varepsilon_{ij} \sim r^{\lambda - 1}$ where the eigenvalue λ is found by solving the

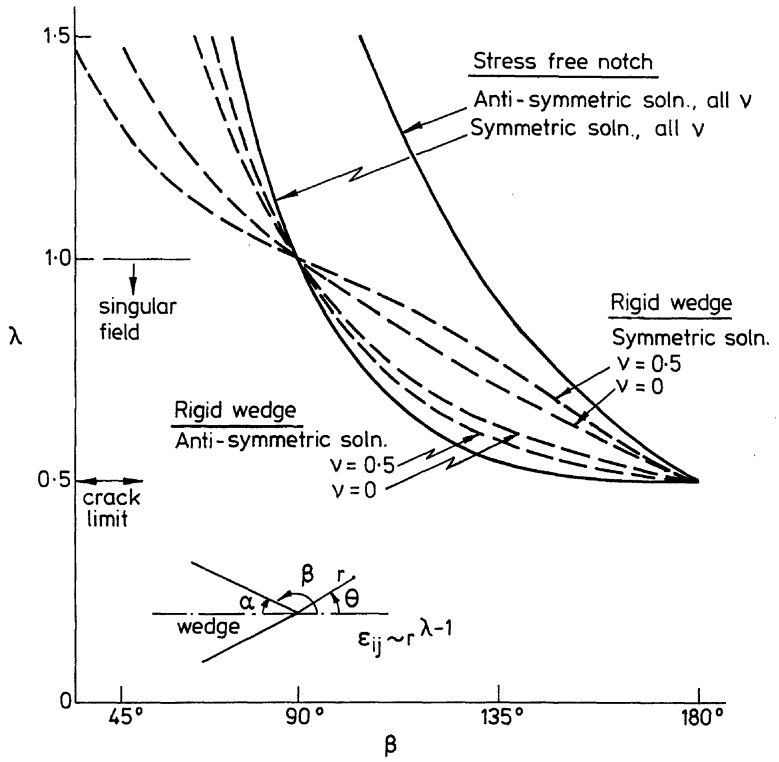

FIG. 1. Level of singularity, λ, for a two-dimensional notch and rigid wedge in a plane elastic body. Plane deformations are assumed.

equilibrium equations, using an elastic constitutive law, compatibility of strains and traction-free boundary conditions on the wedge. Two independent solutions exist for each geometry, β. Consider polar co-ordinates r, θ centred at the apex of the wedge, as defined in Fig. 1. A symmetric solution exists where the tangential displacement u_θ is even in θ about $\theta = 0$, and an anti-symmetric solution exists where u_θ is odd in θ, see Fig. 1.

For both solutions, the level of strain singularity $(1-\lambda)$ is independent of Poisson's ratio ν, as expected for plane problems with stress boundary conditions. The symmetric solution is singular for a wedge angle $\beta > 90°$: the level of singularity increases from $\lambda = 1$ to $\lambda = 0.5$, as β is increased from the half space geometry, $\beta = 90°$, to the crack limit, $\beta = 180°$. The anti-symmetric solution becomes singular at $\beta = 129°$, and again the level of singularity increases to the value for a crack, $\lambda = 0.5$, as β is increased to 180°.

Now consider the rigid wedge with zero displacement on its flanks. Both the symmetric and anti-symmetric solutions depend on Poisson's ratio ν, and are therefore different for plane stress and for plane strain conditions. The plane strain results for $\nu = 0$ and $\nu = 0.5$ are given in Fig. 1. For both symmetries, the solution becomes increasingly singular (i.e. λ decreases) as the wedge angle β is increased from the clamped half space, $\beta = 90°$, to the limit of a rigid wedge of zero thickness, $\beta = 180°$. For β in the range 90°–180°, the singularity becomes stronger as ν is increased from zero to the incompressible limit of 0.5 for anti-symmetric loading, while the singularity becomes weaker for symmetric loading. It is further noted from

Fig. 1 that the anti-symmetric solution is more singular than the symmetric solution for the rigid wedge, while the reverse holds for the stress-free notch.

Little is known about the strain field near the tip of a stress-free notch or rigid wedge in a rigid-plastic plane body under symmetric or anti-symmetric loading. HUTCHINSON (1968a) considered the specific case of a stress-free notch of included angle $2\alpha = 90°$ in a power hardening body with stress exponent $n = 3$. He found $\varepsilon_{ij} \sim r^{-0.675}$ for the notch under symmetric loading, while $\varepsilon_{ij} \sim r^{-0.75}$ for a crack in the same material; thus, the crack solution is more singular than the notch solution. DUVA (1988) has explored the singular symmetric field at the apex of a square rigid wedge ($2\alpha = 90°$), embedded in an incompressible power law solid. For all n, the singularity is less strong than for the case of a crack.

Recently, ORE and DURBAN (1988) and ATKINSON and CHAMPION (1984) have considered a stress-free notch in an incompressible power law deformation solid under anti-plane shear. They found that the level of strain singularity increases as the included notch angle 2α is decreased to the crack limit, $\alpha = 0$. For a given α, the strain field becomes more singular as n increases to the rigid perfectly-plastic limit, $n = \infty$.

1.2. *The conical notch and rigid cone*

BAZANT and KEER (1974) have examined the local field near the tip of a conical notch and of a rigid cone in a compressible elastic body. They found that no singularity exists for either inhomogeneity under torsion, but a singularity does exist for torsionless axisymmetric loading.

Bazant and Keer suggested a separation of variables solution in terms of spherical polar co-ordinates (r, θ, ϕ) centred on the cone tip, and considered axisymmetric loadings such that the solution is independent of the circumferential angle, ϕ. The co-ordinates (r, θ) are defined on a meridian plane in the insert of Fig. 2. Bazant and

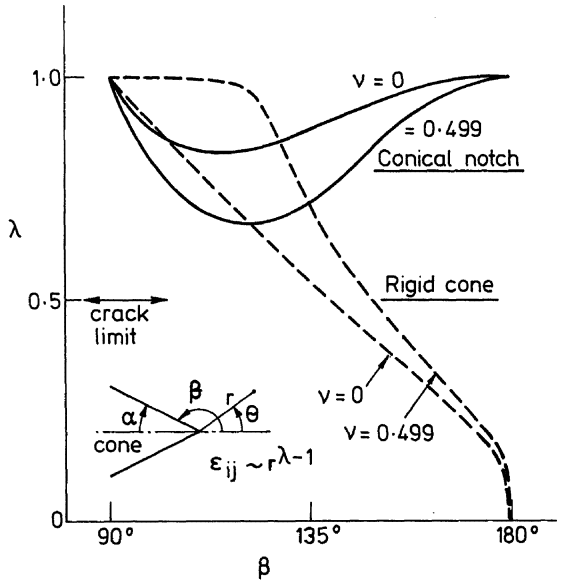

FIG. 2. Level of singularity, λ, for a conical notch and a rigid cone in an elastic body, under torsionless axisymmetric loading.

Keer assumed that the strain field near the apex of the cone behaves as $\varepsilon_{ij} \sim r^{\lambda-1}$, where the eigenvalue λ is less than unity for singular behaviour.

Consider their results for a conical notch under torsionless axisymmetric loading, see Fig. 2. As the apex angle β is increased from 90° to 180°, the cone evolves in shape from a half plane to a needle cavity of zero width. For both limits no singularity exists and $\lambda = 1$, while at intermediate values of β the solution is singular. In contrast with the two-dimensional wedge case (Fig. 1), the strength of the singularity increases to a maximum at $\beta \approx 120°$ and then decreases again as β increases to the needle limit of $\beta = 180°$. For any given β between 90° and 180°, λ decreases as Poisson's ratio ν increases from 0 to 0.499. This contrasts with the solution for a 2D notch where λ is independent of ν. Bazant and Keer did not examine the incompressible limit $\nu = 0.5$.

Now consider a rigid cone under torsionless axisymmetric loading (Fig. 2). As β increases from 90° to 180°, the solution becomes increasingly singular and λ decreases from unity to zero. Since λ equals 0.5 for the case of a crack, we deduce that the solution is more singular than the crack case for $\beta \gtrsim 145°$. We refer to this condition as "supercritical" because there is a strong tendency for a crack to develop from such an inhomogeneity. The level of singularity decreases (i.e. λ increases) as ν is increased from zero to 0.499. This differs from the solution for the conical notch but agrees with the symmetric solution for a 2D rigid wedge.

2. Conical Inhomogeneity in a Power Law Incompressible Material under Torsion

We now examine the asymptotic field at the tip of a conical notch and of a rigid cone, under remote torsion about the axis of the cone. First, an eigenvalue problem is set up for a conical notch and for a rigid cone, in an incompressible power law material under remote torsion. The equations are then specialised and solved for the linear case.

Consider an incompressible power law solid, which obeys the small strain deformation theory of plasticity, such that the strain ε_{ij} is related to the stress σ_{ij} according to

$$\varepsilon_{ij} = \frac{3}{2}\left(\frac{\sigma_{\text{eff}}}{\sigma_0}\right)^n \frac{S_{ij}}{\sigma_{\text{eff}}}. \tag{2.1}$$

Here, $S_{ij} = \sigma_{ij} - \frac{1}{3}\delta_{ij}\sigma_{kk}$ is the deviatoric stress, $\sigma_{\text{eff}} = \sqrt{(3/2)S_{ij}S_{ij}}$ is the effective stress, and σ_0 and the strain hardening exponent n are material constants.

The cone geometry, with spherical polar co-ordinates (r, θ, ϕ) centred at the apex of the cone, is given in Fig. 3. Remote torsion is applied about the $\theta = 0$ centre line, inducing the displacement $u_\phi = w(r, \theta)$ in the ϕ direction. By symmetry there is no warping and $u_r = u_\theta = 0$. The non-vanishing strains associated with these displacements are

$$\varepsilon_{r\phi} = \frac{1}{2}\left(w_{,r} - \frac{w}{r}\right), \tag{2.2a}$$

$$\varepsilon_{\theta\phi} = \frac{1}{2}\left(\frac{1}{r}w_{,\theta} - \frac{w}{r}\cot\theta\right), \tag{2.2b}$$

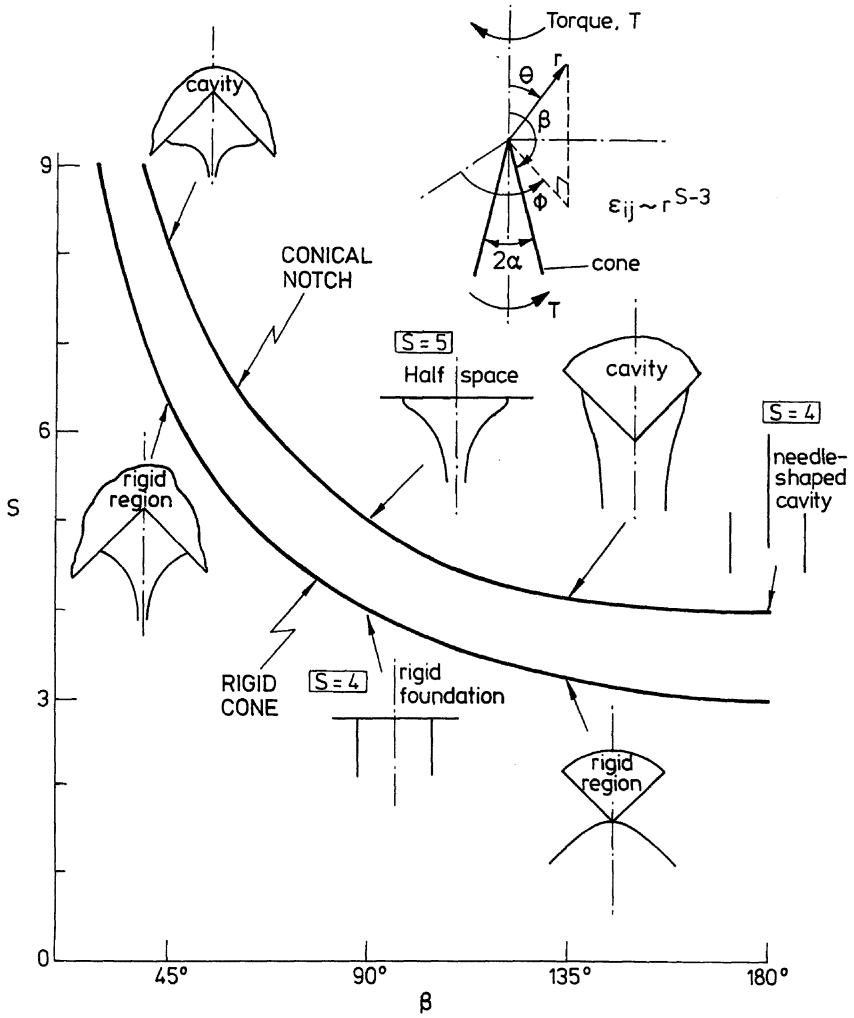

FIG. 3. Solution for conical notch and rigid cone in an incompressible elastic body under remote torsion. Typical contour of effective stress is included for each geometry.

where the comma subscript denotes differentiation with respect to the subscript variable. The strain–displacement relations reduce to the compatibility equation,

$$r\varepsilon_{\theta\phi,r} - (\sin\theta)\left(\frac{\varepsilon_{r\phi}}{\sin\theta}\right)_{,\theta} = 0. \tag{2.2c}$$

The coaxiality of ε_{ij} and σ_{ij} in (2.1) implies that only $\sigma_{r\phi}$ and $\sigma_{\theta\phi}$ are active. The equilibrium equation

$$r\sigma_{r\phi,r} + 3\sigma_{r\phi} + \sigma_{\theta\phi,\theta} + 2\sigma_{\theta\phi}\cot\theta = 0 \tag{2.3}$$

is satisfied if a stress function $F(r, \theta)$ is introduced, where

$$\sigma_{r\phi} = \frac{1}{r^3 \sin^2\theta} F_{,\theta}, \tag{2.4a}$$

$$\sigma_{\theta\phi} = \frac{-1}{r^2 \sin^2\theta} F_{,r}. \tag{2.4b}$$

Now make the assumption that the near tip field is governed asymptotically as $r \to 0$ by a separation of variables solution of the form

$$F = r^s \phi(\theta), \tag{2.5}$$

where s and $\phi(\theta)$ remain to be determined. From Eqs (2.1), (2.4a,b) and (2.5) the strains are

$$\varepsilon_{r\phi} = \frac{3^{\frac{n+1}{2}}}{2} \frac{1}{\sigma_0^n} r^{(s-3)n} \frac{(\phi'^2 + s^2\phi^2)^{\frac{n-1}{2}}}{(\sin\theta)^{2n}} \phi', \tag{2.6a}$$

$$\varepsilon_{\theta\phi} = \frac{-3^{\frac{n+1}{2}}}{2} \frac{1}{\sigma_0^n} r^{(s-3)n} \frac{(\phi'^2 + s^2\phi^2)^{\frac{n-1}{2}}}{(\sin\theta)^{2n}} s\phi, \tag{2.6b}$$

where the prime denotes differentiation with respect to θ. When these expressions for ε_{ij} are substituted into the compatibility equation (2.2c), a non-linear second order, ordinary differential equation results in ϕ,

$$(n-1)(\phi'' + s^2\phi)\phi'^2 + [\phi'' - (2n+1)(\cot\theta)\phi' + s(s-3)n\phi](\phi'^2 + s^2\phi^2) = 0. \tag{2.7}$$

2.1. *Homogeneous case*

It may easily be verified that for $s = 3 + (1/n)$, Eq. (2.7) has the solution

$$\phi(\theta) = C(\sin\theta)^{3+(1/n)}, \tag{2.8}$$

where C is a constant. The stresses associated with this solution are

$$\sigma_{r\phi} = C\left(3 + \frac{1}{n}\right) r^{1/n} (\sin\theta)^{1/n} \cos\theta, \tag{2.9a}$$

$$\sigma_{\theta\phi} = -C\left(3 + \frac{1}{n}\right) r^{1/n} (\sin\theta)^{1+(1/n)}. \tag{2.9b}$$

This solution describes torsion of a circular bar (KACHANOV, 1971).

2.2. *Torsion of a circular conical bar*

For the case $s = 0$, Eq. (2.7) has the solution

$$\phi' = C(\sin\theta)^{\frac{2n+1}{n}}, \tag{2.10}$$

where C is a constant. The associated stresses are

$$\sigma_{r\phi} = \frac{C}{r^3} (\sin\theta)^{1/n}, \tag{2.11a}$$

$$\sigma_{\theta\phi} = 0. \tag{2.11b}$$

This is the solution for torsion by a torque T about the axis of a conical cylindrical shaft, of apex angle 2α. The constant C is fixed by T and α.

2.3. *Solution for conical notch and rigid cone in a linear elastic material*

For the case of a conical notch, the stress component $\sigma_{\theta\phi}$ equals zero on the face of the cone, giving the boundary condition

$$\phi = 0 \quad \text{on } \theta = \beta. \tag{2.12a}$$

For the rigid cone, the displacement $u_\phi = w$ equals zero on the face of the cone. It follows from (2.2a) that

$$w = 2r \int \varepsilon_{r\phi} \frac{dr}{r}$$

and by (2.6a),

$$w = \frac{3^{\frac{n+1}{2}}}{\sigma_0^n} \frac{r^{(s-3)n+1}}{(s-3)n} \frac{(\phi'^2 + s^2\phi^2)^{\frac{n-1}{2}}}{(\sin\theta)^{2n}} \phi'.$$

This implies that on the wall of the rigid cone,

$$\phi' = 0 \quad \text{on } \theta = \beta. \tag{2.12b}$$

By now we have a homogeneous second order differential equation (2.7) with one boundary condition (2.12a) or (2.12b). An additional homogeneous boundary condition is required to solve the system for the eigenvalues s and the eigenfunctions ϕ.

Here, we consider the simpler problem of the linear material, $n = 1$, whereby Eq. (2.7) simplifies to,

$$\phi'' - 3(\cot\theta)\phi' + s(s-3)\phi = 0. \tag{2.13}$$

This has the two linearly independent solutions (Section 8.7, GRADSHTEYN and RYZHIK, 1980),

$$\phi = (\sin^2\theta) P_{s-2}^2(\cos\theta), \tag{2.14a}$$

$$\phi = (\sin^2\theta) Q_{s-2}^2(\cos\theta). \tag{2.14b}$$

where P_{s-2}^2 and Q_{s-2}^2 are associated Legendre functions of order 2 and degree $s-2$. As θ tends to zero, $\sigma_{r\phi} = (r^{s-3}\phi'/\sin^2\theta)$ must tend to zero, hence

$$\phi = \phi' = \phi'' = \phi''' = 0 \quad \text{at } \theta = 0 \tag{2.15}$$

and solution (2.14b) is excluded. The first of (2.15) provides the second homogeneous boundary condition for (2.7) or (2.13). The associated Legendre functions are a subclass of the Hypergeometric function, for which a power series expansion exists, see GRADSHTEYN and RYZHIK (1980) for details. Accordingly, the solution (2.14a) may be expressed as

$$\phi = C \sin^4 \theta \left(1 + \sum_{p=3}^{\infty} a_p \sin^{2(p-2)} \frac{\theta}{2}\right), \tag{2.16a}$$

where

$$a_p = \frac{2p(p-1)}{p!p!} \prod_{i=4}^{p+1} (-s+i) \prod_{j=1}^{p-2} (s+j). \tag{2.16b}$$

The lowest eigenvalue s and associated eigenfunction $\phi(\theta)$ which satisfy the boundary conditions (2.12a) or (2.12b) are found from (2.16a) using a Newton–Raphson iteration scheme. For β approaching 180°, the infinite series (2.16a, b) converges slowly and the first 10^3 terms are needed. Only non-singular solutions with $s \geqslant 3$ are found, Fig. 3, as commented by BAZANT and KEER (1974) for the linear, compressible solid.

For both the rigid cone and the conical notch, as β increases the eigenvalue s decreases. At any given β, s is smaller for the rigid cone than for the conical notch, implying that the stress increases more rapidly with increasing r for the rigid cone than for the conical notch.

Typical contours of constant effective stress from the apex of the conical inhomogeneity are included in Fig. 3 for a selection of geometries. The effective stress $\sigma_{\text{eff}} = \sqrt{3}(\sigma_{r\phi}^2 + \sigma_{\theta\phi}^2)^{1/2}$ has the asymptotic representation from (2.4) and (2.5),

$$\sigma_{\text{eff}} = \frac{\sqrt{3} r^{s-3}}{\sin^2 \theta} (\phi'^2 + s^2 \phi^2)^{1/2}.$$

It is thought that this contour of constant σ_{eff} gives an indication of the shape of the elastic–plastic boundary between the elastic region near the axis $\theta = 0$, and the outer plastic region. For $s > 4$, a region of low stress (i.e. small σ_{eff}) extends along the face of the conical notch and of the rigid cone. When β is greater than 90° for the rigid cone, the solution is $s < 4$ and the region of low stress extends ahead of the cone rather than flanking the faces of the cone, see Fig. 3.

For the needle-shaped cavity (conical notch, $\beta = 180°$) and for the rigid half space (rigid cone, $\beta = 90°$) the homogeneous solution (2.9a, b) applies, and $s = 4$. Then, the solution is

$$\sigma_{r\phi} = 4Cr \sin \theta \cos \theta, \tag{2.17a}$$

$$\sigma_{\theta\phi} = -4Cr \sin^2 \theta \tag{2.17b}$$

and contours of constant effective stress are parallel to the axis $\theta = 0$.

Analytic solutions for $\phi(\theta)$ also exist for $s = 3$ and 5. For $s = 3$,

$$\phi = C(\cos \theta)(2 + \sin^2 \theta) \tag{2.18a}$$

and for $s = 5$,

$$\phi = C \sin^4 \theta \cos \theta. \tag{2.18b}$$

The solution for $s = 3$, Eq. (2.18a), is discounted as it predicts unbounded strain energy near $\theta = 0$. For the limiting case of a rigid needle ($\beta \to 180°$), the homogeneous solution given by Eqs (2.9a, b) applies and $s = 4$. This is expected since the stresses

and displacements on $\theta = 0$ are zero for the homogeneous case, prior to introduction of an inhomogeneity in the form of a rigid needle or of a needle-shaped cavity.

The observation of no singularity for conical inhomogeneities in torsion is consistent with the fact that the energy release rate $\mathscr{G}$ at the tip of a propagating circular cylindrical cavity in a bar under torsion is zero. See Appendix A for details.

3. Torsionless Axisymmetric Case

We now examine the asymptotic field near the tip of a conical notch and of a rigid cone, in an incompressible power law material under torsionless axisymmetric loading. As for the torsion case, an eigenvalue problem is posed, where the eigenvalue s denotes the level of singularity. We shall find singular solutions for a range of β and strain hardening exponent n, for both the rigid cone and the conical notch.

First, the field equations are given, then the problem is solved analytically for the linear case $n = 1$, and solved numerically in Section 4 for the non-linear case.

3.1. *Field equations*

Spherical polar co-ordinates (r, θ, ϕ) are used as before, with the geometry specified in Fig. 3. By symmetry, the radial displacement u_r and tangential displacement u_θ depend only on r, θ, and $u_\phi = 0$. The strain–displacement relations are

$$\varepsilon_{rr} = u_{r,r}, \tag{3.1a}$$

$$\varepsilon_{\theta\theta} = \frac{u_r + u_{\theta,\theta}}{r}, \tag{3.1b}$$

$$\varepsilon_{\phi\phi} = \frac{u_r + u_\theta \cot\theta}{r}, \tag{3.1c}$$

$$\varepsilon_{r\theta} = \frac{1}{2}\left(u_{\theta,r} - \frac{u_\theta}{r} + \frac{u_{r,\theta}}{r}\right). \tag{3.1d}$$

From these relations and the constitutive law (2.1), it follows that the active stresses are σ_{rr}, $\sigma_{\theta\theta}$, $\sigma_{\phi\phi}$ and $\sigma_{r\theta}$. Equilibrium in the radial direction reduces to

$$r\sigma_{rr,r} + 2\sigma_{rr} - \sigma_{\theta\theta} - \sigma_{\phi\phi} + \sigma_{r\theta,\theta} + \sigma_{r\theta}\cot\theta = 0, \tag{3.2a}$$

while equilibrium in the tangential direction gives

$$r\sigma_{r\theta,r} + 3\sigma_{r\theta} + \sigma_{\theta\theta,\theta} + (\sigma_{\theta\theta} - \sigma_{\phi\phi})\cot\theta = 0. \tag{3.2b}$$

Substitution of Eqs (3.1a–c) into the incompressibility condition $\varepsilon_{kk} = 0$ yields a differential equation in u_r, u_θ, which is satisfied identically by introducing a stream function $\psi(r, \theta)$ defined by

$$u_r = \frac{\psi_{,\theta}}{r^2 \sin\theta}, \tag{3.3a}$$

$$u_\theta = -\frac{\psi_{,r}}{r \sin\theta}. \tag{3.3b}$$

We try a separation of variables solution for the asymptotic form of ψ as $r \to 0$,

$$\psi = r^s(\sin\theta)\phi(\theta). \tag{3.4}$$

This results in an eigenvalue problem where we seek the lowest eigenvalue $s > 2$ and associated eigenfunction ϕ. The condition $s > 2$ enforces the condition that displacements are zero at the tip of the cone. The solution is singular for $s < 3$.

3.2. *Linear material*

An analytic expression for $\phi(\theta)$ can be found for the linear case, $n = 1$. The displacements u_r, u_θ follow directly from (3.3a,b) and (3.4),

$$u_r = r^{s-2}(\phi' + \phi \cot\theta) \tag{3.5a}$$

and

$$u_\theta = -r^{s-2}(s\phi), \tag{3.5b}$$

where the prime denotes differentiation with respect to θ. The strain components, via (3.1a–d), are

$$\varepsilon_{rr} = r^{s-3}(s-2)(\phi' + \phi \cot\theta), \tag{3.6a}$$

$$\varepsilon_{\theta\theta} = r^{s-3}[(1-s)\phi' + \phi \cot\theta], \tag{3.6b}$$

$$\varepsilon_{\phi\phi} = r^{s-3}[\phi' + (1-s)\phi \cot\theta] \tag{3.6c}$$

and

$$\varepsilon_{r\theta} = \tfrac{1}{2}r^{s-3}[\mathscr{L}(\phi) + s(3-s)\phi], \tag{3.6d}$$

where

$$\mathscr{L}(\phi) \equiv (\phi' + \phi \cot\theta)'. \tag{3.6e}$$

The constitutive relations for a linear elastic incompressible material are

$$\sigma_{rr} - \sigma_h = \varepsilon_{rr}, \quad \sigma_{\theta\theta} - \sigma_h = \varepsilon_{\theta\theta}, \quad \sigma_{\phi\phi} - \sigma_h = \varepsilon_{\phi\phi}, \quad \sigma_{r\theta} = \varepsilon_{r\theta}, \tag{3.7}$$

where $\sigma_h = \frac{1}{3}(\sigma_{rr} + \sigma_{\theta\theta} + \sigma_{\phi\phi})$ is the hydrostatic stress and all stress components have been non-dimensionalised with respect to $\frac{2}{3}\sigma_0 = \frac{2}{3}E$, where E is Young's modulus.

The equilibrium equations (3.2a,b) become

$$r\sigma_{h,r} + r\varepsilon_{rr,r} + 2\varepsilon_{rr} - \varepsilon_{\theta\theta} - \varepsilon_{\phi\phi} + \varepsilon_{r\theta,\theta} + \varepsilon_{r\theta} \cot\theta = 0 \tag{3.8a}$$

and

$$\sigma_{h,\theta}+\varepsilon_{\theta\theta,\theta}+(\varepsilon_{\theta\theta}-\varepsilon_{\phi\phi})\cot\theta+r\varepsilon_{r\theta,r}+3\varepsilon_{r\theta}=0 \tag{3.8b}$$

or, after eliminating σ_h,

$$\left(\varepsilon_{rr,r}+\frac{2\varepsilon_{rr}-\varepsilon_{\theta\theta}-\varepsilon_{\phi\phi}}{r}+\frac{\varepsilon_{r\theta,\theta}+\varepsilon_{r\theta}\cot\theta}{r}\right)_{,\theta}$$

$$-(\varepsilon_{\theta\theta,\theta}+(\varepsilon_{\theta\theta}-\varepsilon_{\phi\phi})\cot\theta+r\varepsilon_{r\theta,r}+3\varepsilon_{r\theta})_{,r}=0. \tag{3.9}$$

Inserting the strains (3.6a–d) into (3.9) and observing (3.6e), gives

$$\mathscr{L}^2(\phi)+2(s^2-3s+3)\mathscr{L}(\phi)+s(s-1)(s-2)(s-3)\phi=0. \tag{3.10a}$$

Two independent solutions to Eq. (3.10a) are found by factorising (3.10a) into

$$(\mathscr{L}-k_1)(\mathscr{L}-k_2)\phi=0, \tag{3.10b}$$

where $k_1=-s(s-1)$ and $k_2=-(s-2)(s-3)$ are the roots of the equation

$$k^2+2(s^2-3s+3)k+s(s-1)(s-2)(s-3)=0. \tag{3.10c}$$

The equation

$$(\mathscr{L}-k)\phi=0 \tag{3.11a}$$

is an associated Legendre equation, with the solution (GRADSHTEYN and RYZHIK, 1980),

$$\phi=P'_\nu(\cos\theta)+Q'_\nu(\cos\theta),\quad \nu(\nu+1)=-k, \tag{3.11b}$$

where P_ν and Q_ν are Legendre functions of degree ν. The solution of Eq. (3.10b) follows immediately as

$$\phi(\theta)=C_1P'_{s-1}(\cos\theta)+C_2P'_{s-3}(\cos\theta), \tag{3.12a}$$

where C_1 and C_2 are arbitrary constants, and the functions $Q'_{s-1}(\cos\theta)$, $Q'_{s-3}(\cos\theta)$ have been neglected on physical grounds as they are unbounded at $\theta=0$.

The first derivatives of the Legendre functions in (3.12a) may be expressed as an infinite power series (GRADSHTEYN and RYZHIK, 1980), as

$$P'_{s-1}(\cos\theta)=\frac{-s(s-1)}{s}\sin\theta\left(1+\sum_{n=2}^{\infty}a_n\sin^{2(n-1)}\frac{\theta}{2}\right),$$

$$a_n=\frac{1}{n!(n-1)!}\prod_{i=2}^{n}(-s+i)\prod_{j=1}^{n-1}(s+j) \tag{3.12b}$$

and

$$P'_{s-3}(\cos\theta)=\frac{-(s-3)(s-2)}{2}\sin\theta\left(1+\sum_{n=2}^{\infty}b_n\sin^{2(n-1)}\frac{\theta}{2}\right),$$

$$b_n=\frac{1}{n!(n-1)!}\prod_{i=4}^{2+n}(-s+i)\prod_{j=-1}^{-3+n}(s+j). \tag{3.12c}$$

The solution for $\phi(\theta)$ in (3.12a) is fully specified, once the eigenvalue s and the ratio

C_2/C_1 are found from the boundary conditions at the surface of the conical notch or of the rigid cone.

3.3. *Boundary conditions, linear material*

3.3.1. *Conical notch.* The surfaces of the conical notch are traction free, hence $\sigma_{\theta\theta}$ and $\sigma_{r\theta}$ are zero at $\theta = \beta$. Note that from (3.7) $\sigma_{\theta\theta} = \sigma_h + \varepsilon_{\theta\theta}$ so we need to evaluate σ_h in order to apply the boundary condition $\sigma_{\theta\theta} = 0$. Integration of (3.8a) with respect to r, using (3.6a–e), gives ($s \neq 3$)

$$\sigma_h = r^{s-3}\left[\frac{-s(s-1)}{2(s-3)}(\phi' + \phi\cot\theta) - \frac{1}{2(s-3)}(\mathscr{L}'(\phi) + \mathscr{L}(\phi)\cot\theta)\right]. \quad (3.13)$$

The stress $\sigma_{\theta\theta}$ follows from (3.6b), (3.7) and (3.13),

$$\sigma_{\theta\theta} = r^{s-3}\left[\frac{-(s^2-3s+6)}{2(s-3)}(\phi' + \phi\cot\theta) - s\phi' - \frac{1}{2(s-3)}(\mathscr{L}'(\phi) + \mathscr{L}(\phi)\cot\theta)\right]. \quad (3.14)$$

By (3.11a,b) we have the identities

$$\mathscr{L}(P'_{s-1}(\cos\theta)) = -s(s-1)P'_{s-1}(\cos\theta) \quad (3.15a)$$

and

$$\mathscr{L}(P'_{s-3}(\cos\theta)) = -(s-2)(s-3)P'_{s-3}(\cos\theta) \quad (3.15b)$$

and $\mathscr{L}(\phi)$ reduces to

$$\mathscr{L}(\phi) = -C_1 s(s-1)P'_{s-1}(\cos\theta) - C_2(s-2)(s-3)P'_{s-3}(\cos\theta). \quad (3.16)$$

Further, note that the Legendre function $P_\nu(\cos\theta)$ satisfies the Legendre equation

$$P''_\nu + P'_\nu\cot\theta + \nu(\nu+1)P_\nu = 0. \quad (3.17)$$

Thus, the condition $\sigma_{\theta\theta} = 0$ in (3.14) may be rewritten via (3.12a), (3.16) and (3.17) as

$$C_1[P''_{s-1}(\cos\theta) + (s-1)P_{s-1}(\cos\theta)] + C_2[P''_{s-3}(\cos\theta) - (s-2)P_{s-3}(\cos\theta)] = 0 \quad \text{at } \theta = \beta. \quad (3.18)$$

Now consider the boundary condition $\sigma_{r\theta} = 0$ at $\theta = \beta$. The constitutive law $\sigma_{r\theta} = \varepsilon_{r\theta}$ and (3.6d) provide the condition in terms of ϕ,

$$\mathscr{L}(\phi) + s(3-s)\phi = 0 \quad \text{at } \theta = \beta. \quad (3.19)$$

Substitution of (3.16) for $\mathscr{L}(\phi)$ leads to the condition

$$C_1[s(s-2)P'_{s-1}(\cos\beta)] + C_2[(s-1)(s-3)P'_{s-3}(\cos\beta)] = 0. \quad (3.20)$$

The two equations (3.18) and (3.20) are satisfied at the surface of the conical notch $\theta = \beta$ by an appropriate choice of s and C_2/C_1. On writing the equations in matrix form $\mathbf{AX} = \mathbf{0}$,

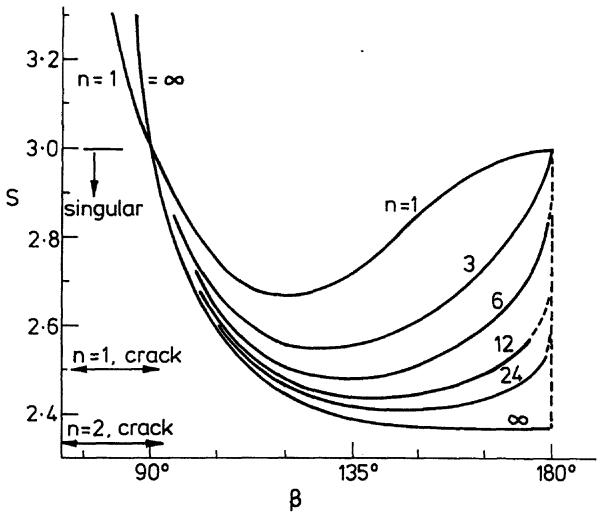

FIG. 4. Level of singularity, s, for a conical notch in an incompressible power law material under torsionless axisymmetric loading. The crack singularities are expressed by $s = 3-n/(n+1)$.

$$\begin{bmatrix} (P''_{s-1}+(s-1)P_{s-1}) & (P''_{s-3}-(s-2)P_{s-3}) \\ (s(s-2)P'_{s-1}) & ((s-1)(s-3)P'_{s-3}) \end{bmatrix} \begin{bmatrix} C_1 \\ C_2 \end{bmatrix} = \begin{bmatrix} 0 \\ 0 \end{bmatrix} \quad \text{at } \theta = \beta, \quad (3.21)$$

it is clear that a solution is found when the determinant of the matrix **A** is zero. For a given β, the equation $\det \mathbf{A} = 0$ is solved iteratively using the Newton–Raphson method. Series expansions are used to evaluate expressions of the form P_ν, P'_ν and P''_ν, as given in (3.12b) and by GRADSHTEYN and RYZHIK (1980). The Newton correction on each iteration is calculated using numerical differentiation.

Computed values of s are plotted against β in Fig. 4. The results are indistinguishable from those given by BAZANT and KEER (1974) for $\nu = 0.499$. Stresses are singular ($s < 3$) for $90° < \beta < 180°$, and the singularity is strongest at $\beta = 120°$.

3.3.2. *Rigid cone.* At the surface of the rigid cone, the displacements u_r and u_θ are zero. These conditions may be rewritten via (3.5a b) and (3.12a) as

$$\begin{bmatrix} P'_{s-1}(\cos\beta) & P'_{s-3}(\cos\beta) \\ P''_{s-1}(\cos\beta) & P''_{s-3}(\cos\beta) \end{bmatrix} \begin{bmatrix} C_1 \\ C_2 \end{bmatrix} = \begin{bmatrix} 0 \\ 0 \end{bmatrix}. \quad (3.22)$$

Again, this system of 2 linear equations is solved for s and C_2/C_1 by putting the determinant of the matrix equal to zero. The same Newton–Raphson procedure and series expansions for P'_ν and P''_ν are used as for the conical notch case. Results are given in Fig. 5.

For $\beta < 120°$, stresses are non-singular ($s > 3$), while for $120° < \beta < 180°$ stresses are singular ($s < 3$). The level of the singularity increases (s decreases) as β is increased to the limit of a rigid needle, $\beta = 180°$. The Bazant and Keer solution for $\nu = 0.499$ lies close to the present solution for $\nu = 0.5$, for $\beta > 120°$, but deviates for smaller values of β. Whereas the Bazant and Keer solution for s asymptotes to $s = 3$ as β is decreased from 120° to 90°, s increases to $s = 4$ at $\beta = 90°$ for the incompressible solid.

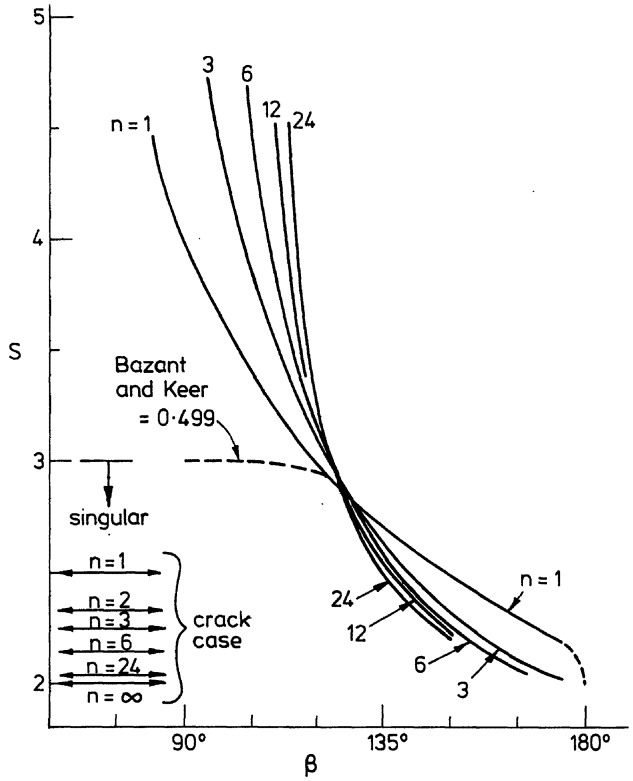

FIG. 5. Level of singularity, s, for a rigid cone in an incompressible power law material under torsionless axisymmetric loading. The crack singularities are expressed by $s = 3-n/(n+1)$.

3.4. *Analytic solution for linear material*, s = 3

When $s = 3$, $\boldsymbol{\sigma}$ is independent of r, and (3.10a) may be solved analytically to give the eigenfunction $\phi(\theta)$,

$$\phi(\theta) = C_1 \sin 2\theta + C_2 \tan \frac{\theta}{2}. \tag{3.23}$$

This solution applies to the case of a rigid cone of angle $\beta = 120°$; a similar development to that leading to (3.22) gives $C_1 = 2C_2$, and $\boldsymbol{\sigma}$ varies with θ but not r. This analytic solution is in agreement with the numerical solution for $\nu = 0.5$, and differs from the Bazant and Keer solution for $\nu = 0.499$.

For the conical notch, (3.23) with $s = 3$ applies to the case of a half space ($\beta = 90°$), and to the limiting case of a needle-shaped cavity ($\beta \to 180°$). For the half space, the solution is homogeneous since $\boldsymbol{\sigma}$ is independent of r and θ; substitution of (3.23) into (3.6a–d), together with the constitutive law (3.7), the equilibrium equation (3.8b), and the boundary condition $\sigma_{r\theta} = \sigma_{\theta\theta} = 0$ at $\theta = 90°$ gives $C_2 = 0$. The stress components are

$$\sigma_{rr} = -6C_1 \sin^2 \theta, \tag{3.24a}$$

$$\sigma_{\theta\theta} = -6C_1 \cos^2 \theta, \tag{3.24b}$$

$$\sigma_{\phi\phi} = -6C_1, \tag{3.24c}$$

$$\sigma_{r\theta} = -3C_1 \sin 2\theta, \tag{3.24d}$$

$$\sigma_h = -4C_1, \tag{3.24e}$$

which represents the case of equibiaxial tension tangential to the free surface of the half space.

The solution for the needle-shaped cavity is derived in a similar manner. The result is

$$\sigma_{rr} = 6C_1 \cos^2 \theta, \tag{3.25a}$$

$$\sigma_{\theta\theta} = 6C_1 \sin^2 \theta, \tag{3.25b}$$

$$\sigma_{\phi\phi} = 0, \tag{3.25c}$$

$$\sigma_{r\theta} = -3C_1 \sin 2\theta, \tag{3.25d}$$

$$\sigma_h = 2C_1. \tag{3.25e}$$

This stress state is uniaxial tension in the direction $\theta = 0$. Again the stress state is homogeneous, independent of r and θ.

4. Non-linear Case

The asymptotic stress field near the tip of a conical notch and of a rigid cone is now given, for torsionless axisymmetric loading and the incompressible power law material specified by (2.1). The equilibrium equations (3.2a,b), and strain–displacement relations (3.1a–d) apply as before. Since the material is incompressible, the displacements u_r, u_θ are related to the stream function $\psi(r, \theta)$ by (3.3a,b). Again $\psi(r, \theta)$ is assumed to have the asymptotic form $\psi = r^s(\sin\theta)\phi(\theta)$, Eq. (3.4), for small r.

We seek the lowest eigenvalue $s > 2$ and associated eigenfunction $\phi(\theta)$ as functions of β and n, for the conical notch and the rigid cone. To solve the eigenvalue problem, the governing fourth order non-linear differential equation for ϕ is written as a system of four first order ordinary differential equations of the form

$$y_i' = f_i(\theta, \{y_i\}), \quad i = 1, 2, 3, 4, \tag{4.1}$$

where the first derivatives $y_i' \equiv \mathrm{d}y_i/\mathrm{d}\theta$ $(i = 1, 2, 3, 4)$ of the dependent variables y_i are known functions f_i of θ and $\{y_i\}$. This system of equations is integrated numerically and the boundary conditions at $\theta = 0$, β are used to find s.

4.1. *Governing system of ordinary differential equations*

The governing system of first order differential equations follows naturally from the incompressibility requirement, the strain–displacement relations and from equilibrium.

The displacements u_r, u_θ are expressed via (3.3a,b) in terms of the stream function $\psi = r^s(\sin\theta)\phi(\theta)$,

$$u_r = \frac{\psi_{,\theta}}{r^2 \sin\theta} = r^{s-2}X, \tag{4.2a}$$

$$u_\theta = -\frac{\psi_{,r}}{r \sin\theta} = -sr^{s-2}\phi, \tag{4.2b}$$

where

$$X = \phi' + \phi \cot\theta. \tag{4.2c}$$

The strain components are derived from these displacements using (3.1a–d),

$$\varepsilon_{rr} = u_{r,r} = r^{s-3}(s-2)X, \tag{4.3a}$$

$$\varepsilon_{\theta\theta} = \frac{u_r + u_{\theta,\theta}}{r} = r^{s-3}((1-s)X + s\phi \cot\theta), \tag{4.3b}$$

$$\varepsilon_{\phi\phi} = \frac{u_r + u_\theta \cot\theta}{r} = r^{s-3}(X - s\phi \cot\theta), \tag{4.3c}$$

$$\varepsilon_{r\theta} = \frac{1}{2}\left(u_{\theta,r} - \frac{u_\theta}{r} + \frac{u_{r,\theta}}{r}\right) = r^{s-3}Y, \tag{4.3d}$$

where

$$Y = \tfrac{1}{2}(X' + s(3-s)\phi). \tag{4.3e}$$

A measure Γ of the effective strain ε_{eff} is defined by

$$\varepsilon_{\text{eff}} = \sqrt{\frac{2}{3}\varepsilon_{ij}\varepsilon_{ij}} = \frac{2}{\sqrt{3}} r^{s-3}\Gamma. \tag{4.4a}$$

Substitution of the strain components (4.3a–d) into (4.4a) gives Γ in terms of ϕ, X and Y,

$$\Gamma^2 = (s^2 - 3s + 3)X^2 - s^2(X - \phi \cot\theta)\phi \cot\theta + Y^2. \tag{4.4b}$$

The stress components $\sigma_{ij} = S_{ij} + \sigma_h \delta_{ij}$ follow from inversion of the constitutive law (2.1),

$$\frac{S_{ij}}{\sigma_0} = \frac{2}{3}(\varepsilon_{\text{eff}})^{\frac{1-n}{n}} \varepsilon_{ij} \tag{4.5}$$

together with (4.3a–d), giving

$$\sigma_{rr} - \sigma_h = \frac{\sigma_0}{\sqrt{3}}\left(\frac{2}{\sqrt{3}}\right)^{\frac{1}{n}} r^{\frac{s-3}{n}} \Gamma^{\frac{1-n}{n}} (s-2)X, \tag{4.6a}$$

$$\sigma_{\theta\theta} - \sigma_h = \frac{\sigma_0}{\sqrt{3}}\left(\frac{2}{\sqrt{3}}\right)^{\frac{1}{n}} r^{\frac{s-3}{n}} \Gamma^{\frac{1-n}{n}} ((1-s)X + s\phi \cot\theta), \tag{4.6b}$$

$$\sigma_{\phi\phi}-\sigma_h=\frac{\sigma_0}{\sqrt{3}}\left(\frac{2}{\sqrt{3}}\right)^{\frac{1}{n}} r^{\frac{s-3}{n}}\Gamma^{\frac{1-n}{n}}(X-s\phi\cot\theta) \tag{4.6c}$$

and

$$\sigma_{r\theta}=\frac{\sigma_0}{\sqrt{3}}\left(\frac{2}{\sqrt{3}}\right)^{\frac{1}{n}} r^{\frac{s-3}{n}}\Gamma^{\frac{1-n}{n}} Y. \tag{4.6d}$$

The equilibrium equation (3.2a) suggests that a suitable representation of the hydrostatic stress $\sigma_h(r,\theta)$ is

$$\sigma_h=\frac{\sigma_0}{\sqrt{3}}\left(\frac{2}{\sqrt{3}}\right)^{\frac{1}{n}}[r^{\frac{s-3}{n}}\Gamma^{\frac{1-n}{n}} Z(\theta)+g(\theta)\ln r+D_0], \tag{4.7}$$

where the non-dimensional functions $Z(\theta)$ and $g(\theta)$ remain to be found, and D_0 is a scaling constant. Equations (4.6a–d) and (4.7) are substituted into the equilibrium equations (3.2a and b), giving

$$Y'-\left(\frac{n-1}{n}\right)Y\frac{\Gamma'}{\Gamma}+Y\cot\theta+(s-2)\left(3+\frac{s-3}{n}\right)X+\left(\frac{s-3}{n}\right)Z+r^{\frac{3-s}{n}}\Gamma^{\frac{n-1}{n}} g=0 \tag{4.8a}$$

and

$$Z'+(1-s)X'+s\phi'\cot\theta+\frac{1-n}{n}(Z+(1-s)X+s\phi\cot\theta)\frac{\Gamma'}{\Gamma}+\left(\frac{s-3}{n}+3\right)Y$$
$$+s\phi(\cot^2\theta-1)-sX\cot\theta+g'\Gamma^{\frac{n-1}{n}} r^{\frac{3-s}{n}}\ln r=0. \tag{4.8b}$$

For (4.8b) to remain valid for all r, $g'(\theta)$ vanishes, giving $g(\theta)=D$, a constant. If $s=3$ or $n=\infty$, the exponent in r in (4.8a) vanishes, and the last term in (4.8a) becomes $D\Gamma^{(n-1)/n}$. Then, for the rigid cone, D forms an unknown eigenvalue of the problem; for the conical notch, the boundary condition $\sigma_{\theta\theta}=0$ on $\theta=\beta$ implies via (4.6b) and (4.7) that the constant D vanishes.

Consider the general case, $s\neq 3$ and $n\neq\infty$. For (4.8a) to remain valid for all r, $g=D$ vanishes. We have now a system of 4 first order differential equations in ϕ, X, Y, Z, from (4.2c), (4.3e), (4.8a) and (4.8b), rewritten as

$$\phi'=X-\phi\cot\theta, \tag{4.9a}$$

$$X'=2Y-s(3-s)\phi, \tag{4.9b}$$

$$Y'=-X\left(\frac{(s-2)(s-3)}{n}+3(s-2)\right)-\left(\frac{s-3}{n}\right)Z-Y\cot\theta-\left(\frac{1-n}{n}\right)Y\frac{\Gamma'}{\Gamma}, \tag{4.9c}$$

$$Z'=s(s-2)^2\phi+\left(2s-5-\frac{s-3}{n}\right)Y-\left(\frac{1-n}{n}\right)(Z+(1-s)X+s\phi\cot\theta)\frac{\Gamma'}{\Gamma}. \tag{4.9d}$$

Here, Γ' is expressible in terms of ϕ', X' and Y' by differentiation of (4.4b) with respect to θ. The system of 4 equations (4.9a–d) may be written symbolically as,

$$\begin{bmatrix} \phi' \\ X' \\ Y' \\ Z' \end{bmatrix} = f_i(\theta, \phi, X, Y, Z), \quad i = 1, 2, 3, 4, \tag{4.10}$$

in accordance with (4.1).

We find the lowest eigenvalue $s > 2$ by integrating the system of equations (4.10) from the pole $\theta = 0$ to the boundary $\theta = \beta$. The correct value of s satisfies the boundary conditions.

4.1.1. *Behaviour near pole.* As $\theta \to 0$, $u_\theta \to 0$ because of material continuity. By symmetry $\sigma_{r\theta} \to 0$ as $\theta \to 0$, and by the equilibrium equation (3.2b) we must have $(\sigma_{\theta\theta} - \sigma_{\phi\phi}) \to 0$ in order for the term $(\sigma_{\theta\theta} - \sigma_{\phi\phi})\cot\theta$ to remain bounded.

The presence of $\cot\theta$ in the governing system of equations (4.9a–d) means that the numerical solution is ill-conditioned at $\theta = 0$. Accordingly, the equations are integrated from a small positive value of $\theta = 1°$, using asymptotic approximations for ϕ, X, Y, Z at small θ. These analytic approximations are obtained as follows.

The dependent variables ϕ and Z are analytic for small θ,

$$\phi = a_0 + \theta + a_1\theta^2 + a_2\theta^3 + \cdots, \tag{4.11a}$$

$$Z = b_1 + b_2\theta + b_3\theta^2 + b_4\theta^3 + \cdots, \tag{4.11b}$$

where we put arbitrarily the coefficient in front of the θ term for ϕ to unity, since the governing equations and boundary conditions are homogeneous. Expressions for $X = \phi' + \phi\cot\theta$ and $Y = \frac{1}{2}(X' + s(3-s)\phi)$ are generated directly from (4.11a).

The behaviour at the pole $\theta = 0$, and the equilibrium equations impose conditions on the coefficients a_i, b_i of (4.11a,b). As $\theta \to 0$, $u_\theta = -sr^{s-2}\phi \to 0$, which implies that $a_0 = 0$ in (4.11a). Further, as $\theta \to 0$, $\sigma_{r\theta} \to 0$, hence $Y \to 0$ by (4.6d) and $a_1 = 0$ from examination of the power series expansion of $Y(\theta)$. The condition $(\sigma_{\theta\theta} - \sigma_{\phi\phi}) \to 0$ as $\theta \to 0$ is satisfied identically when $\sigma_{\theta\theta}$ and $\sigma_{\phi\phi}$ are expressed as power series in θ via (4.6b,c) and (4.11a).

The power series for ϕ, X, Y and Z are substituted into the equilibrium equations (4.8a,b) where we consider the general case $s \neq 3$ and $n \neq \infty$, such that $g(\theta) = D$ vanishes. Collected terms in successive powers in θ are put equal to zero in order to satisfy equilibrium. This gives

$$b_1 = \frac{2n}{3-s}\left(4a_2 - \frac{1}{3} + \frac{1}{2}s(3-s) + (s-2)\left(3 + \frac{s-3}{n}\right)\right) \tag{4.12a}$$

and

$$b_2 = 0, \tag{4.12b}$$

where a_2 is unknown from the behaviour near $\theta = 0$ and becomes one of the unknown parameters to be determined. Near $\theta = 0$, the series (4.11a) and (4.11b) reduce to

$$\phi(\theta) = \theta + a_2\theta^3 + O(\theta^5), \tag{4.13a}$$

$$X(\theta) = 2 + (4a_2 - \tfrac{1}{3})\theta^2 + O(\theta^4), \tag{4.13b}$$

$$Y(\theta) = \left(\frac{s(3-s)}{2} + 4a_2 - \frac{1}{3}\right)\theta + O(\theta^3), \tag{4.13c}$$

$$Z(\theta) = \frac{2n}{3-s}\left(4a_2 - \frac{1}{3} + \frac{1}{2}s(3-s) + (s-2)\left(3 + \frac{s-3}{n}\right)\right) + O(\theta^2). \tag{4.13d}$$

Thus, for small θ, the dependent variables ϕ, X, Y, Z can be expressed in terms of the two unknown parameters s and a_2. At $\theta = \beta$ the traction boundary condition $\sigma_{\theta\theta} = \sigma_{r\theta} = 0$ for the conical notch, or the displacement boundary condition $u_r = u_\theta = 0$ for the rigid cone, imposes 2 constraints on $\phi(\beta)$, $X(\beta)$, $Y(\beta)$, and $Z(\beta)$. This leaves 2 of the 4 dependent variables at $\theta = \beta$ as unknown parameters, A_1 and A_2. We have, therefore, a two point boundary value problem consisting of 4 first order differential equations with 4 unknown parameters s, a_2, A_1 and A_2. The numerical procedure for solution of this eigenvalue problem is now given, first for the conical notch and then for the rigid cone.

4.2. *Solution for conical notch*

At the surface of the conical notch the stress components $\sigma_{\theta\theta}$ and $\sigma_{r\theta}$ are zero. This boundary condition in $\sigma_{\theta\theta}$ may be expressed in terms of ϕ, X, Y and Z via (4.6b) and (4.7) to give

$$(1-s)X + s\phi \cot\theta + Z = 0, \quad \theta = \beta, \tag{4.14a}$$

while the boundary condition in $\sigma_{r\theta}$, via (4.6d), gives

$$Y = 0, \quad \theta = \beta. \tag{4.14b}$$

The values $X(\beta) = A_1$, $Z(\beta) = A_2$ form unknown parameters of the problem in addition to s and a_2.

The two point boundary value problem consisting of the differential equations (4.9a–d), the boundary conditions (4.13a–d) at $\theta = 1°$, and the boundary conditions given above at $\theta = \beta$, is solved using a commercially available numerical package developed by the Numerical Algorithms Group. Using initial guessed values of the unknown parameters s, a_2, A_1 and A_2, the system of differential equations is integrated numerically from $\theta = 1°$ to $\theta = \beta$ using the Runge–Kutta–Merson method. Corrected values of the parameters are calculated using a generalised Newton iteration method. The Newton correction in each iteration is determined using a Jacobian matrix whose (i, j)th element depends on the derivative of the ith component of the solution $y_i = (\phi, X, Y, Z)$ with respect to the jth parameter $p_j = (s, a_2, A_1, A_2)$. This matrix is calculated by numerical differentiation. This process is repeated iteratively until convergence is obtained. A form of parameter tracking is used whereby the previous converged

solution of the parameters p_i is used to give the starting value for successively larger values of n or β.

The lowest eigenvalue $s > 2$ is given as a function of β, for various n values in Fig. 4. Results for the linear case $n = 1$ are in agreement with the solution presented in Section 3. It is clear that for $\beta > 90°$, stresses are singular at the tip of the cone. For any fixed n, the singularity is strongest at a value of β which increases from 120° for $n = 1$, to 180° for $n \to \infty$. For a given $\beta > 90°$, the level of singularity increases (i.e. s decreases) as n increases. For all β, the solution is less singular than for a plane crack, where for any type of loading $s = 3-n/(n+1)$ (HUTCHINSON, 1968a,b; RICE and ROSENGREN, 1968). In this sense, the conical notch is less damaging than a plane crack.

4.2.1. *Rigid perfectly-plastic limit.* Figure 4 includes the rigid perfectly-plastic limit, $n = \infty$. The governing system of 4 first order differential equations is now derived for this case. The constitutive law (4.5) reduces to

$$\frac{S_{ij}}{\sigma_0} = \frac{2}{3}\frac{\varepsilon_{ij}}{\varepsilon_{\text{eff}}}, \tag{4.15}$$

where σ_0 is identified with the uniaxial yield stress. The stress components (4.6a–d, 4.7) become

$$\sigma_{rr} - \sigma_h = \frac{\sigma_0}{\sqrt{3}}(s-2)\frac{X}{\Gamma}, \tag{4.16a}$$

$$\sigma_{\theta\theta} - \sigma_h = \frac{\sigma_0}{\sqrt{3}}\frac{((1-s)X + s\phi\cot\theta)}{\Gamma}, \tag{4.16b}$$

$$\sigma_{\phi\phi} - \sigma_h = \frac{\sigma_0}{\sqrt{3}}\frac{(X - s\phi\cot\theta)}{\Gamma}, \tag{4.16c}$$

$$\sigma_{r\theta} = \frac{\sigma_0}{\sqrt{3}}\frac{Y}{\Gamma} \tag{4.16d}$$

and

$$\sigma_h = \frac{\sigma_0}{\sqrt{3}}\frac{Z}{\Gamma}. \tag{4.16e}$$

The effective strain measure Γ is still given by (4.4b), and the system of differential equations governing ϕ, X, Y and Z (4.9a–d) simplifies to

$$\phi' = X - \phi\cot\theta, \tag{4.17a}$$

$$X' = 2Y - s(3-s)\phi, \tag{4.17b}$$

$$Y' = -3(s-2)X - Y\cot\theta + Y\frac{\Gamma'}{\Gamma}, \tag{4.17c}$$

$$Z' = s(s-2)^2\phi + (2s-5)Y + (Z + (1-s)X + s\phi \cot\theta)\frac{\Gamma'}{\Gamma}. \tag{4.17d}$$

A solution is found using (4.17a–d) instead of (4.9a–d), with the boundary conditions unchanged. This solution is included in Fig. 4. It is apparent that the rigid perfectly-plastic case gives the most singular solution at any given β.

4.2.2. *Case* s = 3. Equations (4.17a–d) with (4.12a,b) remain well-behaved and may be integrated for the non-singular limit $s = 3$.

4.2.3. *Discussion of results for conical notch.* Contours of constant effective stress σ_{eff} are given in Fig. 6 for conical notches of angle $\beta = 95°$, 135° and 175°, and various n. The stresses are normalised according to (HUTCHINSON, 1968a),

$$\sigma_{ij}(r,\theta) = r^{\frac{s-3}{n}}\tilde{\sigma}_{ij}(\theta) \tag{4.18a}$$

where $\tilde{\sigma}_{ij}(\theta)$ is deduced from (4.6 and 4.7), consistent with

$$(\tilde{\sigma}_{\text{eff}}(\theta))_{\max} = 1, \quad 0 \leqslant \theta \leqslant \beta. \tag{4.18b}$$

The tilde components give the polar profile of the stress field after normalisation such that $[\sigma_{\text{eff}}(r = 1, \theta)]_{\max} = 1$.

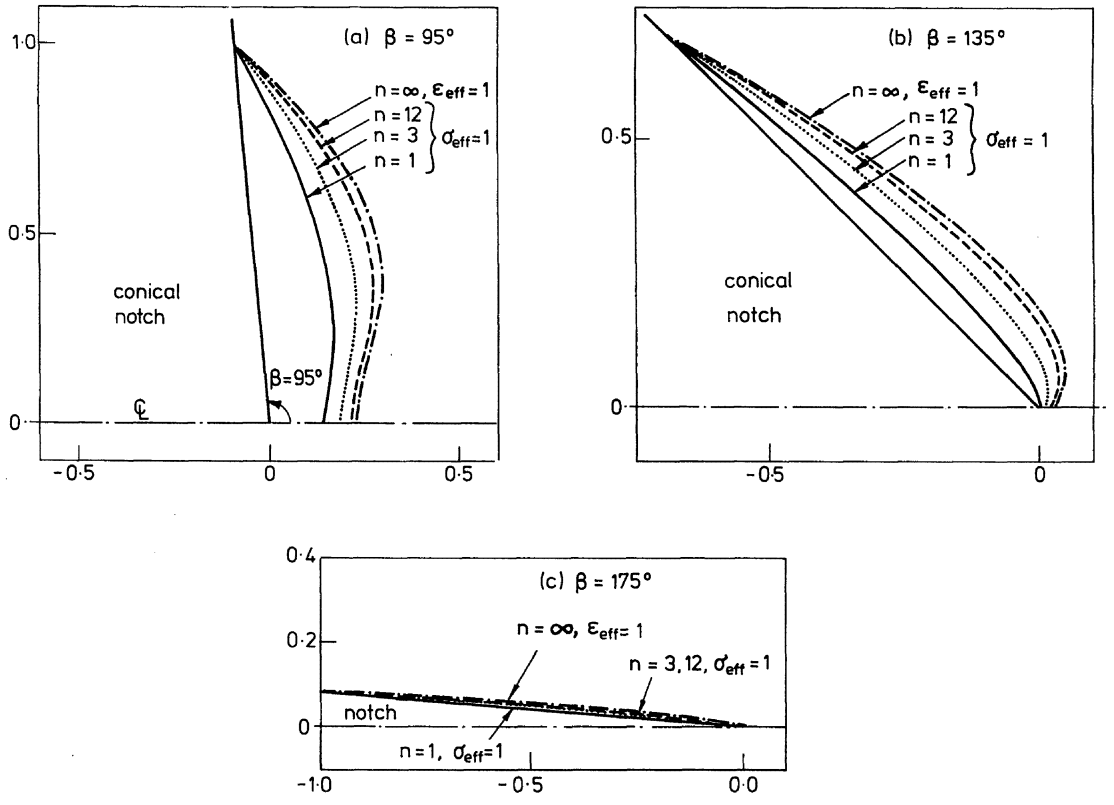

FIG. 6. Plot of constant $\sigma_{\text{eff}}(r, \theta)$ at tip of conical notch for (a) $\beta = 95°$, (b) $\beta = 135°$ and (c) $\beta = 175°$. For $n = \infty$, plot is of constant $\varepsilon_{\text{eff}}(r, \theta)$. Singular solution in all cases.

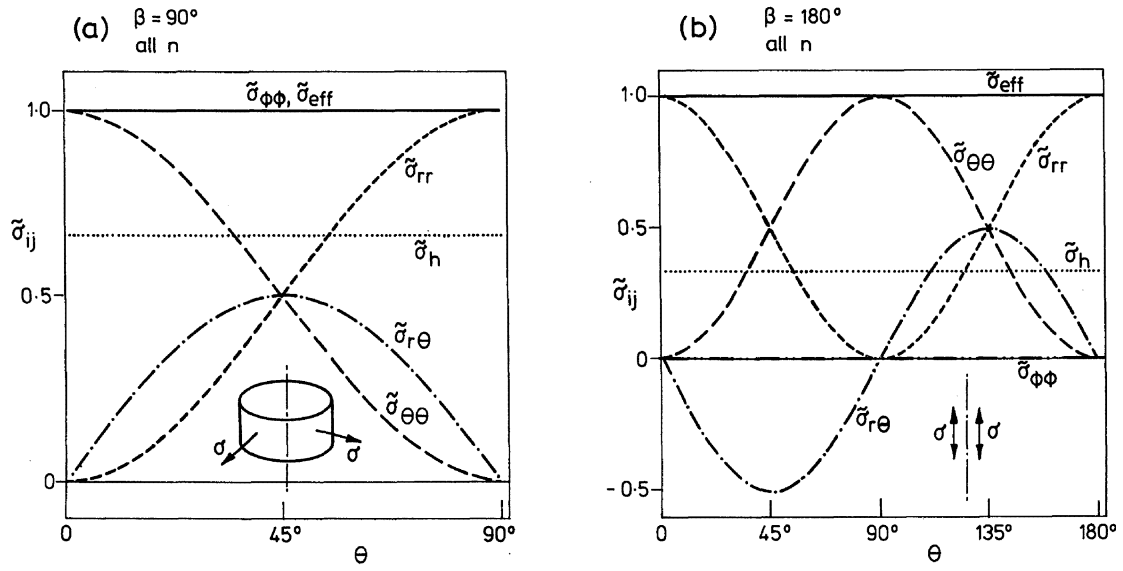

FIG. 7. Stress components $\tilde{\sigma}_{ij}(\theta)$ at tip of conical notch for the special cases (a) half space, $\beta = 90°$, and (b) needle shaped, $\beta = 180°$. All n. All solutions are non-singular with $s = 3$.

Contours of constant effective stress $\sigma_{\text{eff}} = r^{(s-3)/n}\tilde{\sigma}_{\text{eff}}(\theta)$ equal to unity are given in Fig. 6 for finite n. These contours of constant stress are also contours of constant effective strain, ε_{eff}. For the case of $n = \infty$, $\sigma_{\text{eff}} = \sigma_0$ is uniform for all (r, θ) while $\varepsilon_{\text{eff}} = (2/\sqrt{3})r^{s-3}\Gamma(\theta)$ varies with r and θ. Thus, for $n = \infty$, contours of constant $\varepsilon_{\text{eff}}(r, \theta) = 1$ are included in Fig. 6, where $\varepsilon_{\text{eff}}(r, \theta)$ is normalised such that $[\varepsilon_{\text{eff}}(r = 1, \theta)]_{\max} = 1$, for $0 \leqslant \theta \leqslant \beta$.

For all notch geometries $90° < \beta < 180°$ and all n, stresses are singular at the tip of the cone. The contours of constant σ_{eff} or ε_{eff} give an indication of the shape of the plastic zone at the tip of the conical notch. For all β and n considered in Fig. 6, it appears that the contour of constant σ_{eff} lies close to the surface of the cone, rather than extending deep into the material. The distance from the cone tip to the contour is always less along $\theta = 0$ than along $\theta = \beta$.

The shape of the contour of constant σ_{eff} is strongly dependent on β, but only weakly dependent on n. As β is increased the contour lies closer to the surface of the cone, until at $\beta = 175°$ the contour suggests a boundary layer solution over the surface of the cone.

For $\beta = 90°$ and $180°$, s equals 3 for all n, and the effective stress is uniform. This prevents us from drawing contours of constant effective stress for these geometries. The case $\beta = 90°$ represents a half space under equibiaxial tension parallel to the free surface, while $\beta = 180°$ represents the case of a needle-shaped cavity in a full space, under uniaxial tension parallel to the axis of the needle. These stress states are shown in Fig. 7, and are given analytically by Eqs (3.24) and (3.25) for all n.

The stress components $\tilde{\sigma}_{ij}(\theta)$ corresponding to the geometries and n values of Fig. 6 are displayed in Fig. 8. Consider first $\beta = 95°$ and $n = 1$, 3, 12 and ∞. Since the geometry is close to a half space, the stress field is close to the half space solution of equibiaxial tension, compare Figs 8a and 7a. The effective stress $\tilde{\sigma}_{\text{eff}}(\theta)$ varies little from unity, and the hydrostatic stress $\tilde{\sigma}_h(\theta)$ is equal to 0.7 ± 0.1 for all θ and n, compared to 2/3 for the half space solution.

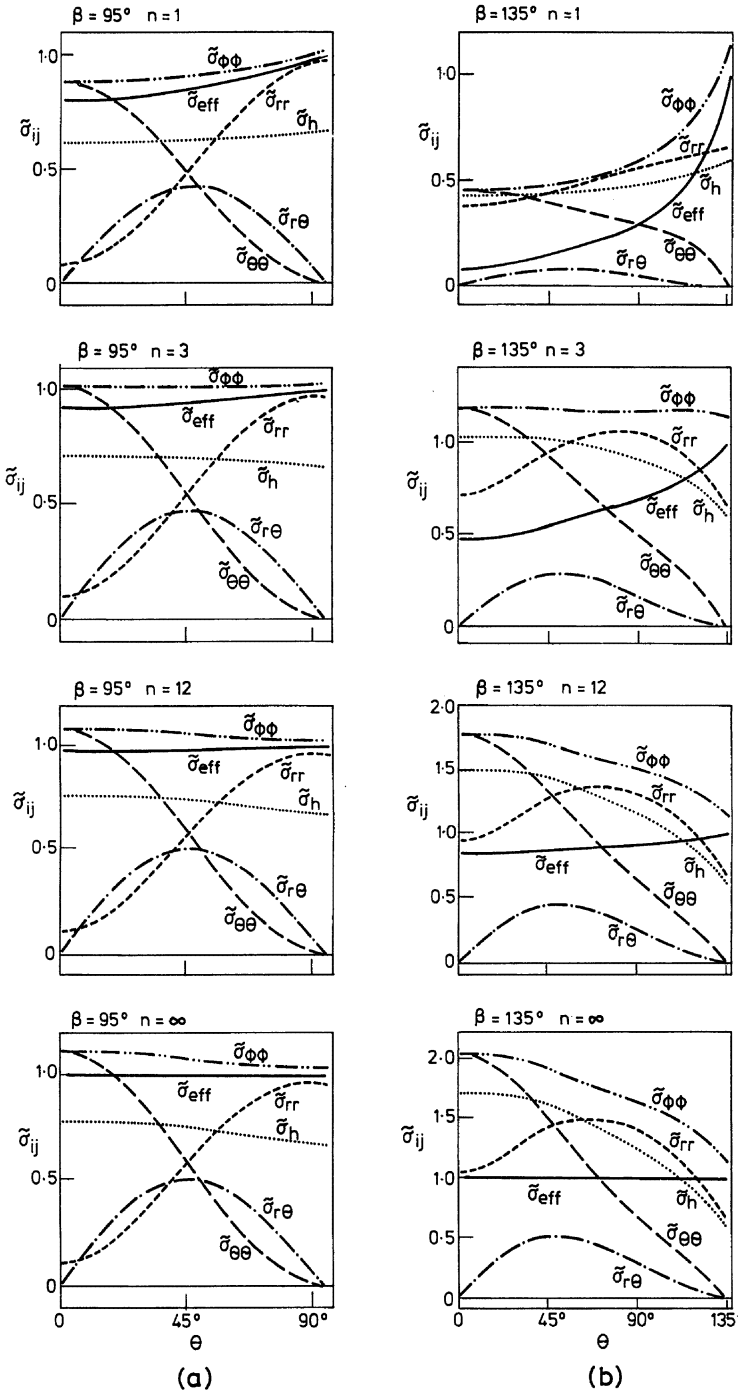

FIG. 8. Stress components $\tilde{\sigma}_{ij}(\theta)$ at tip of conical notch for (a) $\beta = 95°$, (b) $\beta = 135°$ and (c) $\beta = 175°$. For each geometry, $n = 1$, 3, 12 and ∞.

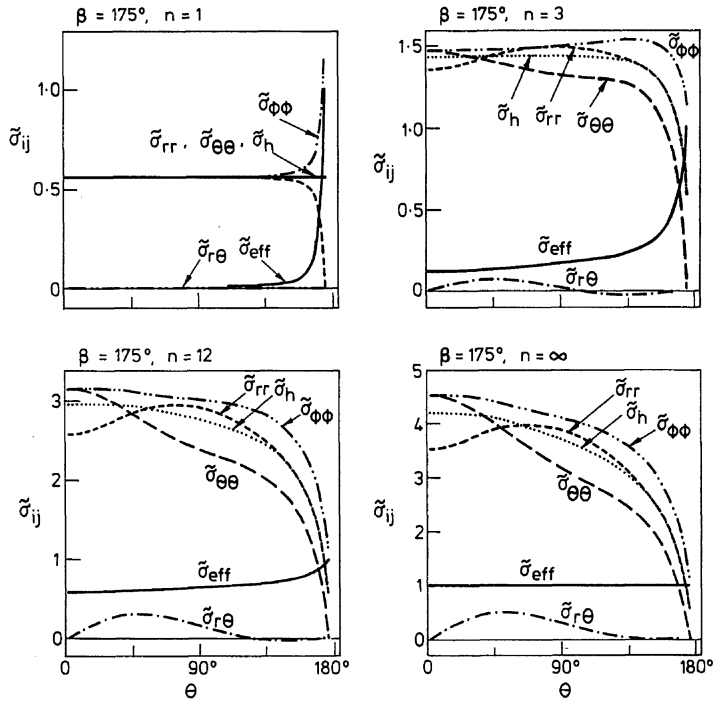

(c)

FIG. 8. (*continued*).

Now consider $\beta = 135°$. For $n = 1$, the effective stress $\tilde{\sigma}_{\text{eff}}$ increases from 0.07 at $\theta = 0°$ to unity at $\theta = \beta$, implying that yielding is preferred along the flanks of the cone. At the surface of the cone $\tilde{\sigma}_{\phi\phi} = 1.1$, $\sigma_{rr} = 0.6$ and $\sigma_{\theta\theta} = \sigma_{r\theta} = 0$, so yielding occurs essentially in the ϕ–θ plane driven by the large 'hoop stress' component $\tilde{\sigma}_{\phi\phi}$. The hydrostatic stress $\tilde{\sigma}_h$ is approximately constant, and equal to 0.5 ± 0.1. As n is increased, the response is qualitatively the same, except for the behaviour of $\tilde{\sigma}_h$. The hydrostatic stress $\tilde{\sigma}_h$ at $\theta = 0$ increases with increasing n, from 0.4 for $n = 1$ to 1.7 for $n = \infty$. As θ is increased to $\theta = \beta$, $\tilde{\sigma}_h$ changes in a monotonic manner to a value of ~ 0.6, for all n. In summary, for this geometry and all n, $\tilde{\sigma}_h$ is larger than $\tilde{\sigma}_{\text{eff}}$ for $\theta = 0°$, while at $\theta = \beta$, $\tilde{\sigma}_h \sim 0.6$ is less than $\tilde{\sigma}_{\text{eff}} = 1$ and yielding is by the 'hoop stress' component $\tilde{\sigma}_{\phi\phi}$.

The behaviour for $\beta = 175°$ and all n shows the same trends as for $\beta = 135°$, but in a more extreme fashion. Except for $n = \infty$, the effective stress $\tilde{\sigma}_{\text{eff}}$ remains small until θ approaches β; as θ tends to β, $\tilde{\sigma}_{\text{eff}}$ increases rapidly to a value of unity at $\theta = \beta$. The stress state changes from essentially hydrostatic at $\theta = 0°$, to tensile yielding in the ϕ-direction at $\theta = \beta$. The magnitude of $\tilde{\sigma}_h$ at $\theta = 0°$ increases from 0.56 to 4.2 as n is increased from unity to infinity. This result for $\tilde{\sigma}_h$ along $\theta = 0°$ in the rigid perfectly-plastic material is unusually large: the corresponding crack problem under Mode I loading gives a value of $(\tilde{\sigma}_h)_{\max} = (2+\pi)/\sqrt{3} = 2.97$ ahead of the crack tip.

4.3. *Solution for rigid cone*

Consider the asymptotic stress field near the tip of a rigid cone in a power law incompressible material under remote torsionless axisymmetric loading. The governing differential equations (4.9a–d) apply when $s \neq 3$ and $n \neq \infty$, with the behaviour

at small θ still given by (4.13a–d). At the surface of the rigid cone the displacements u_r, u_θ are zero and (4.2a,b) imply

$$\phi(\beta) = 0, \tag{4.19a}$$

$$X(\beta) = 0. \tag{4.19b}$$

The dependent variables $Y(\beta) = A_1$ and $Z(\beta) = A_2$ become the unknown parameters of the problem, in addition to s and a_2.

The same solution procedure is used as for the case of the conical notch. The governing differential equations (4.9a–d) are integrated numerically from $\theta = 1°$ to $\theta = \beta$ and values for s, a_2, A_1, A_2 are found which satisfy the boundary conditions at each end of the integration interval. Results for the eigenvalue s as a function of β are shown in Fig. 5, for a range of n.

It is clear from Fig. 5 that for a fixed n the solution becomes increasingly singular (s decreases) as β increases. The value of β at which the solution becomes singular ($s = 3$) increases slightly from 120° as n is increased from unity. For $\beta \gtrsim 120°$, the level of singularity increases (s decreases) with increasing n, while the reverse is true for $\beta \lesssim 120°$. At any given n, the solution is more singular than the crack solution $s = 3 - n/(n+1)$, for β sufficiently close to the rigid needle limit of $\beta = 180°$.

Convergence to a stable solution was neither achieved for β near 180°, nor for the limit $n \to \infty$.

4.3.1. *Discussion of results for rigid cone.* Contours of constant $\sigma_{\text{eff}}(r, \theta)$ are given in Fig. 9 for the case of a rigid cone and $\beta = 90°$, 95°, 135° and 175°. Behaviour is more complex than for the conical notch, as the value of β at which stresses become singular depends on n, see Fig. 5.

In all cases, the contour of constant σ_{eff} lies close to the surface of the rigid cone rather than extending deep into the material: the distance from the tip of the cone to the contour of constant σ_{eff} is always greater along $\theta = \beta$ than along $\theta = 0°$. For $\beta \lesssim 120°$ and all n, stresses are non singular and the contour of constant σ_{eff} only gives an approximate indication of the shape of the plastic zone surrounding the tip of the rigid cone.

The normalised stresses $\tilde{\sigma}_{ij}(\theta)$ for the cases given in Fig. 9 are shown in Fig. 10. In all cases the stress state along $\theta = \beta$ consists of pure shear with hydrostatic tension: $\tilde{\sigma}_{r\theta}$ is finite, and $\tilde{\sigma}_{rr} = \tilde{\sigma}_{\theta\theta} = \tilde{\sigma}_{\phi\phi} = \tilde{\sigma}_h$. Along $\theta = 0$, $\tilde{\sigma}_{r\theta}$ is zero and $\tilde{\sigma}_{\theta\theta}$ equals $\tilde{\sigma}_{\phi\phi}$ by the equilibrium equations (3.2a) and (3.2b), respectively. The stress state along $\theta = 0$ thus reduces to axisymmetric tension $\tilde{\sigma}_{\theta\theta} = \tilde{\sigma}_{\phi\phi}$ with an algebraically larger stress $\tilde{\sigma}_{rr}$.

For $\beta \lesssim 120°$, stresses are non singular and $\tilde{\sigma}_{\text{eff}}(\theta)$ attains its maximum value of unity at $\theta = 0$. For larger β, stresses become singular and $\tilde{\sigma}_{\text{eff}}(\theta)$ equals unity at $\theta = \beta$. The magnitude of the hydrostatic stress $\tilde{\sigma}_h$ increases with increasing θ for all β, n. Its magnitude at $\theta = \beta$ varies in a complicated manner with β and n, and attains a maximum value $\tilde{\sigma}_h \sim 6$ for $\beta = 135°$, $n = 12$.

Now consider the plots of $\tilde{\sigma}_{ij}(\theta)$ and contours of $\tilde{\sigma}_{\text{eff}}$ in more detail for each selected β value. Consider first the results for $\beta = 90°$, $n = 1$. This represents a clamped half space, bonded to a rigid foundation. The non-singular stress state at $\theta = \beta$ consists of pure shear $\tilde{\sigma}_{r\theta}$ with zero hydrostatic stress (Fig. 10a). The cases $\beta = 95°$, $n = 1, 3$ are similar, and $|\tilde{\sigma}_h| = 0.1$–0.2 is small at $\theta = \beta$. The associated contours of constant

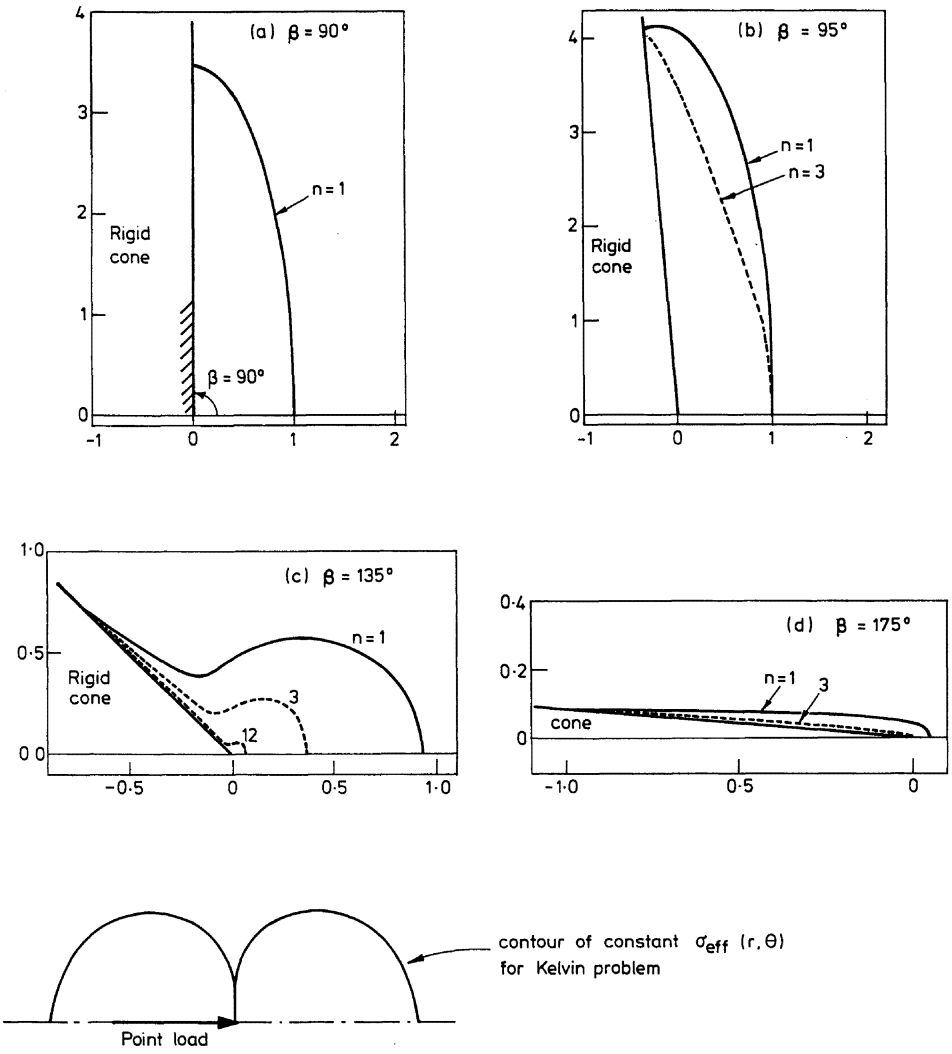

FIG. 9. Plot of constant $\sigma_{\text{eff}}(r, \theta)$ at tip of rigid cone for (a) $\beta = 90°$ (solution is non-singular), (b) $\beta = 95°$ (solutions are non-singular), (c) $\beta = 135°$ (solutions are singular) and (d) $\beta = 175°$ (solutions are singular).

σ_{eff} for these two geometries resemble those for the conical notch with $\beta = 95°$, $n = 1$ to ∞, compare Figs 6 and 9.

Stresses remain non singular for the case $\beta = 120°$. An analytic solution has been already given in Section 3.4 for this geometry and the linear material. The eigenvalue s equals 3, and $\phi(\theta)$ follows from (3.23) as

$$\phi = 2C_2 \sin 2\theta + C_2 \tan\frac{\theta}{2}, \tag{4.20}$$

where C_2 is an arbitrary constant. The deviatoric stresses are obtained from (3.6)–(3.7) in the form

$$\sigma_{rr} - \sigma_h = \frac{2}{3}\sigma_0 \varepsilon_{rr} = \frac{2}{3}\sigma_0 C_2 (9 - 12\sin^2\theta), \tag{4.21a}$$

$$\sigma_{\theta\theta} - \sigma_h = \frac{2}{3}\sigma_0 \varepsilon_{\theta\theta} = \frac{2}{3}\sigma_0 C_2 \left(12\sin^2\theta - \frac{9}{2} - \frac{3}{2}\tan^2\frac{\theta}{2}\right), \tag{4.21b}$$

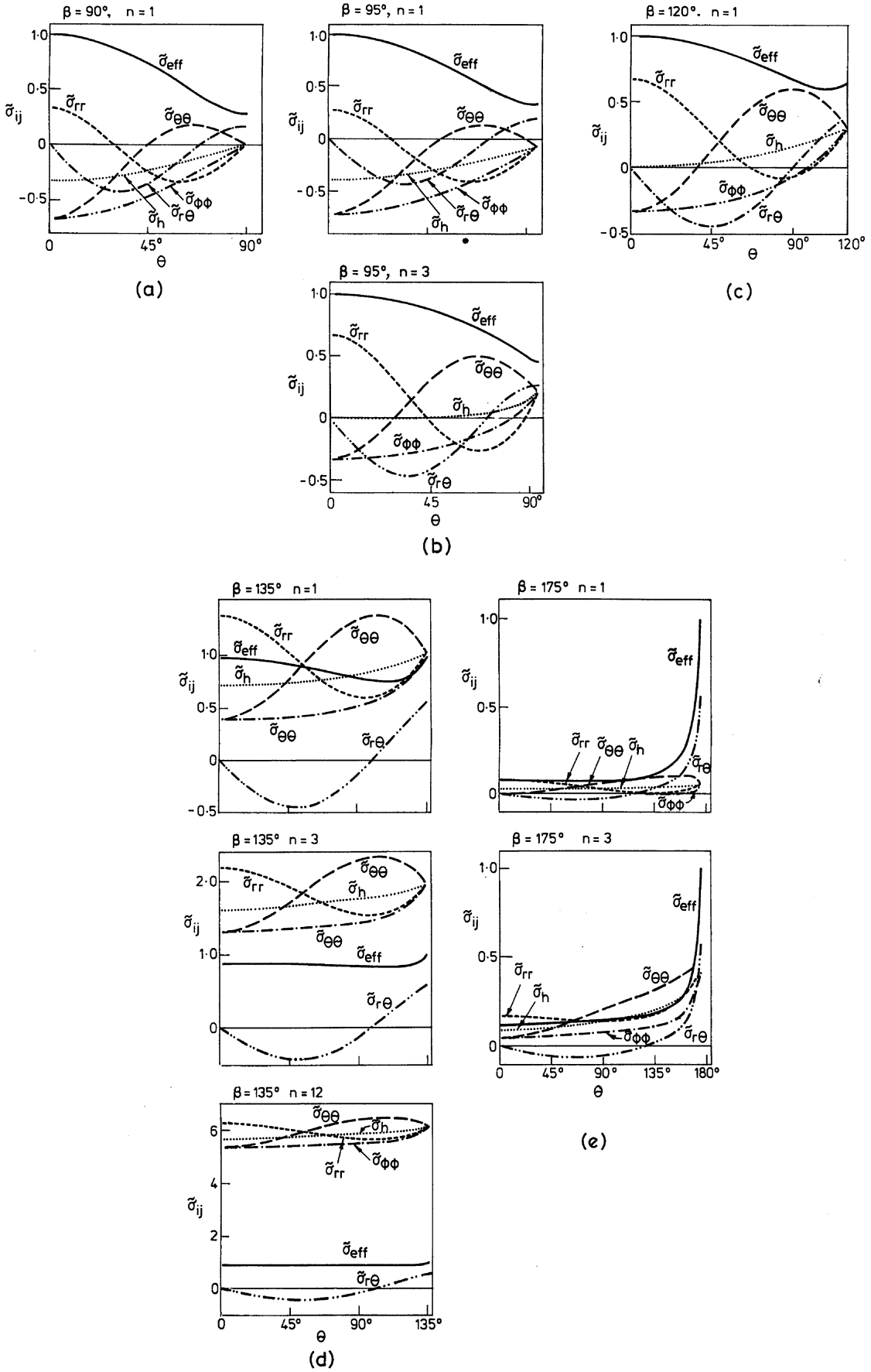

FIG. 10. Stress components $\tilde{\sigma}_{ij}(\theta)$ at tip of rigid cone for (a) $\beta = 90°$ (non-singular solution), (b) $\beta = 95°$ (non-singular solutions), (c) $\beta = 120°$ (non-singular solution), (d) $\beta = 135°$ (singular solutions), and (e) $\beta = 175°$ (singular solutions).

$$\sigma_{\phi\phi} - \sigma_h = \frac{2}{3}\sigma_0 \varepsilon_{\phi\phi} = \frac{2}{3}\sigma_0 C_2 \left(-\frac{9}{2} + \frac{3}{2}\tan^2 \frac{\theta}{2} \right), \tag{4.21c}$$

$$\sigma_{r\theta} = \frac{2}{3}\sigma_0 \varepsilon_{r\theta} = \frac{2}{3}\sigma_0 C_2 (-6 \sin 2\theta). \tag{4.21d}$$

The hydrostatic stress σ_h is specialised from (4.7) as

$$\sigma_h(r, \theta) = \frac{2}{3}\sigma_0 \left[Z(\theta) + D \ln \frac{r}{r_0} \right], \tag{4.22a}$$

where r_0 is a new scaling constant, replacing D_0 in (4.7). Substitution of (4.21a–d) and (4.22) for the stresses into the equilibrium equation (3.2a) gives $g(\theta) = -3C_2$, while substitution for the stresses into the second equilibrium equation (3.2b) gives

$$Z(\theta) = -6C_2 \ln \left(\cos \frac{\theta}{2} \right). \tag{4.22b}$$

Thus σ_h is expressed by

$$\sigma_h(r, \theta) = \frac{2}{3}\sigma_0 C_2 \left[-6 \ln \left(\cos \frac{\theta}{2} \right) - 3 \ln \frac{r}{r_0} \right]. \tag{4.23}$$

We note from (4.21a–d) that the deviatoric stresses and the strains are independent of r, while σ_h depends upon r via the ln r term in (4.23). The stress components σ_{ij} are plotted in Fig. 10c, for the choice $r = r_0$, and $C_2 = 1/9\sigma_0$ such that $[\sigma_{\text{eff}}(r = r_0, \theta)]_{\max} = 1$. The effective stress $\sigma_{\text{eff}}(r = r_0, \theta)$ shows a small deviation from unity as θ is increased from zero to β. Since deviatoric stresses are independent of r, a contour of constant $\sigma_{\text{eff}}(r, \theta)$ is a ray along $\theta = 0$.

Now consider the case $\beta = 135°$, for which the solution is singular in r for all n considered. The effective stress $\tilde{\sigma}_{\text{eff}}(\theta)$ is approximately unity except for θ near 110° where it drops slightly in value. This behaviour gives rise to the unusual shape of the constant $\sigma_{\text{eff}}(r, \theta)$ contours (Fig. 9). The contours penetrate far into the material at $\theta = 0°$, engulfing the tip of the cone. The nearest point between the contours and the tip of cone is $\theta \sim 110°$; at larger values of θ the contours flank the surface of the rigid cone. The shape of the contours ahead of the cone is reminiscent of that for a point load, P, applied to an elastic full space, the Kelvin problem (see, for example, TIMOSHENKO and GOODIER, 1970). Kelvin's solution gives $\sigma_{\text{eff}}(r, \theta) = r^{-2}\tilde{\sigma}_{\text{eff}}(\theta)$ where $\tilde{\sigma}_{\text{eff}}(\theta) = \cos \theta$ and $\tilde{\sigma}_h = -\frac{1}{3}\cos \theta$. For the incompressible solid, the Kelvin solution also applies to a half space under a normal load $P/2$. A contour of constant $\sigma_{\text{eff}}(r, \theta)$ for the Kelvin problem is included in Fig. 9.

For $\beta = 135°$ and all θ, the hydrostatic stress $\tilde{\sigma}_h$ increases from ~ 1 for $n = 1$ to ~ 6 for $n = 12$. This suggests that the load carried by a conical indenter stuck to the material is supported largely by hydrostatic stress, for the non-linear solid.

Finally, consider the rigid cone with $\beta = 175°$, $n = 1$ and 3. This geometry approaches that of a rigid needle. Stresses are strongly singular: for $n = 1$ s equals 2.19 compared with the case of a planar crack in an elastic solid where $s = 2.5$. As

for the case of a conical notch of $\beta = 175°$, $\tilde{\sigma}_{\text{eff}}(\theta)$ increases from approximately zero to unity only when θ approaches β. The corresponding contours of constant $\sigma_{\text{eff}}(r, \theta)$ flank the surfaces of the rigid cone and of the conical notch, see Figs 9d and 6c.

Acknowledgements

One of us (DD) wishes to express his thanks for the kind hospitality of the Cambridge University Engineering Department during the sabbatical year 1986/87. Part of this research has been supported by the VPR-Aeronautical Engineering Research Fund, Technion, Haifa, Israel.

References

Atkinson, C. and Champion, C. R.	1984	*Q. J. Mechs appl. Math.* **37**,401.
Bazant, Z. P. and Keer, L. M.	1974	*Int. J. Solids Structures* **10**, 957.
Duva, J. M.	1988	*J. appl. Mech.* **55**, 361.
Gradshteyn, I. S. and Ryzhik, I. M.	1980	*Tables of Integrals, Series and Products*, Academic Press, New York.
Hutchinson, J. W.	1968a	*J. Mech. Phys. Solids* **16**, 13.
Hutchinson, J. W.	1968b	*J. Mech. Phys. Solids* **16**, 337.
Kachanov, L. M.	1971	*Foundations of the Theory of Plasticity*, North-Holland Publ., Co., Amsterdam.
Karal, F. C. and Karp, S. N.	1964	*Geophysics* **29**, 360.
Karp, S. N. and Karal, F. C.	1962	*Comm. Pure appl. Math.* **15**, 413.
Ore, E. and Durban, D.	1988	*Int. J. Fracture* **38**, 15.
Rice, J. R. and Rosengren, G. F.	1968	*J. Mech. Phys. Solids* **16**, 1.
Timoshenko, S. P. and Goodier, J. N.	1970	*Theory of Elasticity*, 3rd edn, McGraw-Hill, New York.
Williams, M. L.	1952	*J. appl. Mech.* **19**, 526.

Appendix A
Calculation of Energy Release Rate

A.1. *Bar in tension*

The strain energy release rate $\mathcal{G}$ for a needle-shaped cavity in a long elastic bar in torsion is calculated as follows. Consider a bar of length l, outer radius b, containing a circular cylindrical cavity of length x, radius a, as shown in Fig. A1. The solid portion of the bar is assumed to

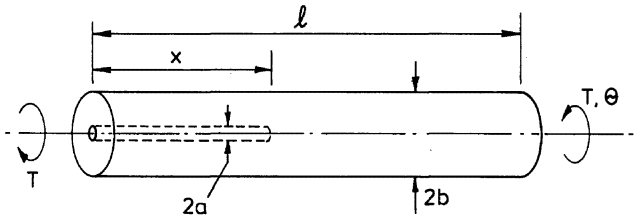

Fig. A1. Calculation of energy release rate $\mathcal{G}$ for advance of a cylindrical hole in a round bar under torsion, or under radial tension.

have torsional rigidity $GJ_1 = \pi G b^4/2$. Treat the hollow portion as a tube with torsional rigidity $GJ_2 = \pi G(b^4 - a^4)/2$, where G is the shear modulus and J_2 is the polar moment of area. If the end rotation of the bar is θ under a torque T, then the compliance $C = \theta/T$ is

$$C \approx \frac{(l-x)}{GJ_1} + \frac{x}{GJ_2}. \tag{A1}$$

The energy release rate $\mathcal{G}$ per unit advance of the hole is given by

$$\mathcal{G} = -\left(\frac{\partial E}{\partial x}\right)_T, \tag{A2a}$$

where $E = -\frac{1}{2}CT^2$ is the potential energy of the body, and T is held constant in the above partial derivative. Hence,

$$\mathcal{G} = \tfrac{1}{2}T^2 \frac{\partial C}{\partial x}. \tag{A2b}$$

Combining Eqs (A1) and (A2b) with the definitions of J_1 and J_2 yields

$$\mathcal{G} \approx \frac{T^2}{\pi G}\left(\frac{1}{b^4 - a^4} - \frac{1}{b^4}\right). \tag{A3}$$

Equation (A3) is exact for the limit $l \to \infty$. For small a/b, (A3) may be rewritten as

$$\mathcal{G} \approx \frac{T^2}{\pi G b^4}\left(\frac{a}{b}\right)^4. \tag{A4}$$

In steady-state hole elongation the energy release rate $\mathcal{G}$ is independent of the details of the shape of the end of the hole, and tends to zero as the hole radius a tends to zero. Thus $\mathcal{G}$ equals zero for the limit of a needle-shaped cavity.

A.2. *Bar under axisymmetric tension*

A similar argument is used to compute $\mathcal{G}$ for a long elastic bar under torsionless axisymmetric tension. Again, consider the geometry given in Fig. A1, with radial tension σ_b applied on the outer surface $r = b$ of the bar (not shown in the figure). When the bar is long, the energy release rate $\mathcal{G}$ is deduced from the difference in potential energy between a solid bar of radius b under σ_b, and a tube of outer radius b, inner radius a, under σ_b. For the solid bar of length $(l-x)$, the potential energy E_1 is

$$E_1 = -\tfrac{1}{2}(2\pi b(l-x))\sigma_b u_{b1}, \tag{A5a}$$

where u_{b1} is the radial displacement at $r = b$ due to σ_b. Similarly for the tube of length x, the potential energy E_2 is

$$E_2 = -\tfrac{1}{2}(2\pi b x)\sigma_b u_{b2}, \tag{A5b}$$

where u_{b2} is the radial displacement at $r = b$.

The displacement u_{b2} is deduced from the well known Lamé equations for a tube, giving

$$u_{b2} = \frac{\sigma_b}{E^*}\frac{b^3}{b^2 - a^2}\left(\frac{(a^2(1+\nu^*) + b^2(1-\nu^*)}{b^2}\right), \tag{A6}$$

where E^*, ν^* are the plane strain values for Young's modulus and Poisson's ratio, respectively. For the solid bar, Eq. (A6) may still be used with the inner radius a put equal to zero.

Combining equation (A6) with (A5a) and (A5b) gives

$$E_1 = -\pi(l-x)\frac{\sigma_b^2}{E^*}b^2(1-\nu^*) \tag{A7a}$$

and

$$E_2 = -\pi x\frac{\sigma_b^2}{E^*}\frac{b^4}{b^2-a^2}\left(\frac{a^2(1+\nu^*)+b^2(1-\nu^*)}{b^2}\right). \tag{A7b}$$

Finally, $\mathcal{G}$ is given by

$$\mathcal{G} = -\frac{\partial(E_1+E_2)}{\partial x}. \tag{A8}$$

Substitution of (A7a,b) into (A8) yields for small a/b,

$$\mathcal{G} \approx 2\pi\frac{\sigma_b^2}{E^*}b^2\left(\frac{a}{b}\right)^2. \tag{A9}$$

For the limiting case of a needle shaped cavity, $a/b \to 0$, and $\mathcal{G} \to 0$ by Eq. (A9).